Journal of Alloys and Compounds 650 (2015) 75–85

Contents lists available at ScienceDirect

Journal of Alloys and Compounds

journal homepage: http://www.elsevier.com/locate/jalcom

Dynamic restoration mechanism and physically based constitutive model of 2050 Al–Li alloy during hot compression

Ruihua Zhu [a], Qing Liu [a], Jinfeng Li [a,*], Sheng Xiang [a], Yonglai Chen [b], Xuhu Zhang [b]

[a] School of Materials Science and Engineering, Central South University, Changsha 410083, China
[b] Aerospace Research Institute of Materials and Processing Technology, Beijing 100076, China

ARTICLE INFO

Article history:
Received 11 May 2015
Received in revised form
17 July 2015
Accepted 19 July 2015
Available online 22 July 2015

Keywords:
2050 Al–Li alloy
Dynamic recrystallization
Dynamic precipitation
σ phase
Particle stimulate nucleation
Constitutive model

ABSTRACT

Dynamic restoration mechanism of 2050 Al–Li alloy and its constitutive model were investigated by means of hot compression simulation in the deformation temperature ranging from 340 to 500 °C and at strain rates of 0.001–10 s^{-1}. The microstructures of the compressed samples were observed using optical microscopy and transmission electron microscopy. On the base of dislocation density theory and Avrami kinetics, a physically based constitutive model was established. The results show that dynamic recovery (DRV) and dynamic recrystallization (DRX) are co-responsible for the dynamic restoration during the hot compression process under all compression conditions. The dynamic precipitation (DPN) of T1 and σ phases was observed after the deformation at 340 °C. This is the first experimental evidence for the DPN of σ phase in Al–Cu–Li alloys. The particle stimulated nucleation of DRX (PSN-DRX) due to the large Al–Cu–Mn particle was also observed. The error analysis suggests that the established constitutive model can adequately describe the flow stress dependence on strain rate, temperature and strain during the hot deformation process.

1. Introduction

The ongoing thrust within the aerospace industry towards reducing structural airframe weight has resulted in the development of Al–Li alloys. Compare to conventional Al alloys, they typically possess lower density, higher elastic modulus and improved fatigue crack growth resistance. 2050 alloy is one of the 3rd generation Al–Li alloys targeting static and fatigue properties to be equal or better than 7050 alloy with 4% density reduction and 5% elastic modulus enhancement [1]. Heretofore, 2050 Al–Li alloy has many applications in transport aircraft from wing spars and ribs to other internal structures in wings and fuselages [2]. These components are usually formed by hot working, either by rolling or forging [3]; the high forming temperatures result in microstructural changes that significantly influence the final mechanical response of the alloy [4]. In view of this, the fundamentals of the themomechanical process, hot deformation characteristics and microstructural evolution accompanying the dynamic restoration process, specific to 2050 Al–Li alloy, need be made clear.

Dynamic recrystallization (DRX) is identified as the key restoration process during microstructural evolution [5,6]. This process, however, is not prone to occur in aluminum and its alloys because of their high stacking fault energy (SFE) [7]. But the formation of new grains of aluminium during hot deformation has been reported frequently [7–10]. Shen et al. [8] revealed the formation of DRX grains during hot compression of an extruded Al–Cu–Li alloy. Hogg et al. [9] indicated that the DRX of the Al–Mg–Li–Zr alloy occurred through nucleation and growth of new grains under the conditions of high temperature and low strain rate. Particle stimulated nucleation of DRX (PSN-DRX) in Al–Mg–Mn alloy due to large particles (>0.6 μm) was observed after the hot deformation [10]. Moreover, many researchers found that dynamic precipitation (DPN) occurred during hot working in 8090 Al–Li alloy [11], 2024 [12] and Al–Mg–Si–Cu alloy [13].

The hot deformation behavior of aluminum alloys is usually characterized by processing factors such as strain, strain rate and deformation temperature. Recently, several empirical, phenomenological and physically based constitutive models have been proposed. Amongst the empirical models, Johnson–Cook (JC) model has been successfully used [14]. However, it is not suitable to represent the flow behavior at temperatures above 0.6 T_m and at lower strain rates [15]. The phenomenological approach [16], in which the flow stress is expressed by the sine-hyperbolic law in an

* Corresponding author.
E-mail address: lijinfeng@csu.edu.cn (J. Li).

http://dx.doi.org/10.1016/j.jallcom.2015.07.182
0925-8388/

Arrhenius-type of equation, has been extensively applied to predict the high-temperature flow behavior. The phenomenological constitutive model, however, does not deeply involve physical mechanisms of materials deformation [17]. Based on the classical stress–dislocation relation and the Avrami kinetics, the physically based constitutive model was established to predict the flow stress for Cu-0.4 Mg alloy [17], steels [18], 7050 Al alloy [19], Nickel-based super-alloy [20] and Al-7.68Zn-2.12Mg-1.98Cu-0.12Zr alloy [21].

In the present study, the hot deformation behavior of 2050 Al–Li alloy based on microstructure evolution as well as true stress-strain curves was studied in detail. Subsequently, the dynamic restoration mechanism of the alloy during hot compression was systematically investigated. Moreover, a physically based constitutive model was developed to reveal the relationship between flow stress and deformation parameters during the whole compression process.

2. Description of the model employed

In the present study, a 0.2% offset in the total strain is used to define the yield stress (σ_0) [21]. The part of each flow curve after "yielding" is fitted with appropriate polynomial using Matlab software [22]. The flow curves are considered to be the net result of the simultaneous operation of dynamic recovery (DRV) and DRX in the manner typified by the schematic curves of Fig. 1. The curve "σ_{DRV}" is regarded as resulting from the operation of DRV alone, i.e. in the absence of DRX. The curve "σ_{DRX}" represents the typical experimental DRX flow curve. Here, DRX is initiated at the critical strain ε_c, after which it leads to more and more softening. The softening attributable to DRX is identified as $\Delta\sigma_s$. The maximum value of $\Delta\sigma_s$ is $\sigma_{sat} - \sigma_{ss}$, where σ_{sat} is the saturation stress of the DRV flow curve, and σ_{ss} is the steady-state stress under DRX conditions. Finally, the fractional softening X_{DRX} is expressed as the following equation [18]:

$$X_{DRX} = \frac{\Delta\sigma_s}{\sigma_{sat} - \sigma_{ss}} = \frac{\sigma_{DRV} - \sigma_{DRX}}{\sigma_{sat} - \sigma_{ss}} \tag{1}$$

2.1. The work hardening model

A dislocation density model [23] is used to describe the work hardening behavior. The model, expressed by Eq. (2), states that the evolution of the dislocation density ρ with strain ε only depends on the current value of ρ via the work hardening parameters h and r. Here, h is the athermal work hardening rate and r specifies the rate of dynamic recovery. Both of them are taken to be strain independent.

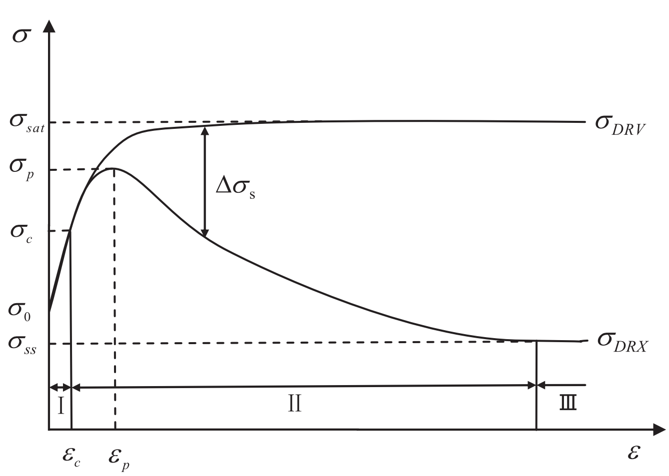

Fig. 1. Schematic diagram illustrating the DRV flow curve and a typical experimental DRX flow curve.

$$\frac{d\rho}{d\varepsilon} = h - r\rho \tag{2}$$

Using the expression $\sigma = \alpha_s G b_s \sqrt{\rho}$, the dislocation density ρ is converted into stress [24]. Here α_s is a dislocation-interaction term, G the shear modulus, and b_s the magnitude of Burger's vector. Finally the dynamic recovery curve can be described as follows (the detailed steps involved in this procedure are described in Ref. [18]):

$$\sigma_{DRV} = \left(\sigma_{sat}^2 - \left(\sigma_{sat}^2 - \sigma_0^2\right)\exp(-r(\varepsilon - \varepsilon_0))\right)^{\frac{1}{2}} \tag{3}$$

2.2. The avrami kinetics

The Avrami formalism is used here to describe the DRX kinetics [18]. This is given by Eq. (4) below, where X is the recrystallized volume fraction, k_s the Avrami constant, q the time exponent, t the recrystallization duration time and $t_{0.5}$ the time for 50% softening.

$$X = 1 - \exp(-k_s t^q) = 1 - \exp\left(-0.693\left(\frac{t}{t_{0.5}}\right)^q\right) \tag{4}$$

In this case, the strain rate is a constant, hence t and $t_{0.5}$ in Eq. (4) can be substituted by $(\varepsilon - \varepsilon_c)/\dot{\varepsilon}$ and $(\varepsilon_{0.5} - \varepsilon_c)/\dot{\varepsilon}$, where $\dot{\varepsilon}$. is the strain rate, ε_c the critical strain, $\varepsilon_{0.5}$ the characteristic strain corresponding to 50% fractional softening. Therefore, the DRX kinetic can be described as:

$$X_{DRX} = 1 - \exp\left(-0.693\left(\frac{\varepsilon - \varepsilon_c}{\varepsilon_{0.5} - \varepsilon_c}\right)^q\right) \quad (\varepsilon \ge \varepsilon_c) \tag{5}$$

2.3. Modeling procedure

In order to model flow curves, the equations for X_{DRX} and σ_{DRV} must be expressed as functions of the Zener-Hollomon parameter $Z = \dot{\varepsilon}\exp\left(\frac{Q}{RT}\right)$, where Q is the deformation activation energy, R the gas constant (8.314 J/(mol K)), T the absolute temperature. For this purpose, the dependences of r, σ_0, σ_{sat}, σ_{ss}, ε_c, $\varepsilon_{0.5}$ and q on Z need to be determined experimentally.

The values of σ_0 and σ_{ss} can be obtained directly from the flow curves. The double differentiation method [25] is used here to calculate the critical strain ε_c. The saturation stress σ_{sat} can be obtained by extrapolation using the experimental results which lies on the flow curve before the critical strain. To determine r, Eq. (3) is rewritten as follow [23]:

$$2\theta\sigma_{DRV} = r\sigma_{sat}^2 - r\sigma_{DRV}^2 \tag{6}$$

which is the tangent equation of the curve shown in Fig. 2, and the value of r can be calculated from the slop. Here θ is the work hardening rate $d\sigma_{DRV}/d\varepsilon$.

3. Experimental material and procedures

The chemical composition (wt. %) of the 2050 Al–Li alloy used in this study was as follows: Cu-3.4, Li-1.2, Mg-0.4, Ag-0.4, Mn-0.35, Zr-0.1, Zn-0.1, Al-bal. The rectangular ingot was homogenized at 450 °C for 16 h and 500 °C for 18 h. Cylindrical specimens with a diameter of 10 mm and a height of 15 mm were machined from the homogenized ingot. Uniaxial compression tests were conducted on a Gleeble-3180D thermal–mechanical simulator (Dynamic Systems Inc., America) in the temperature range from 340 to 500 °C with a